Solar neutrino spectrum, sterile neutrinos, and additional radiation in the Universe

P. C. de Holanda[1] and A. Yu. Smirnov[2]

[1]*Instituto de Física Gleb Wataghin - UNICAMP, 13083-970 Campinas SP, Brazil*

[2]*The Abdus Salam International Centre for Theoretical Physics, I-34100 Trieste, Italy*

(Received 2 February 2011; published 21 June 2011)

Recent results from the SNO, Super-Kamiokande, and Borexino experiments do not show the expected upturn of the energy spectrum of events (the ratio $R \equiv N_{\rm obs}/N_{\rm SSM}$) at low energies. At the same time, cosmological observations testify for the possible existence of additional relativistic degrees of freedom in the early Universe: $\Delta N_{\rm eff} = 1$–2. These facts strengthen the case of a very light sterile neutrino, ν_s, with $\Delta m^2_{01} \sim (0.7\text{–}2) \times 10^{-5}$ eV^2, which mixes weakly with the active neutrinos. The ν_s mixing in the mass eigenstate ν_1 characterized by $\sin^2 2\alpha \sim 10^{-3}$ can explain an absence of the upturn. The mixing of ν_s in the eigenstate ν_3 with $\sin^2\beta \sim 0.1$ leads to production of ν_s via oscillations in the Universe and to additional contribution $\Delta N_{\rm eff} \approx 0.7$–1 before the big bang nucleosynthesis and later. Such a mixing can be tested in forthcoming experiments with the atmospheric neutrinos, as well as in future accelerator long baseline experiments. It has substantial impact on conversion of the supernova neutrinos.

DOI: 10.1103/PhysRevD.83.113011 PACS numbers: 14.60.Pq

I. INTRODUCTION

The large mixing angle (LMA) MSW solution [1,2] has been established as the solution of the solar neutrino problem [3–10]. In assumption of the CPT conservation KamLAND confirms this result [11,12]. One of the main goals of further precision measurements of the solar neutrino fluxes is to search for possible deviations from the LMA predictions which would indicate new physics beyond the standard model with three mixed neutrinos. In particular, new physics can show up at the neutrino energies $E = (1\text{–}7)$ MeV, i.e. in the transition region between the matter dominated conversion and vacuum oscillations. Here, direct measurements of the spectrum are absent or imprecise and possible deviations from the LMA predictions can be relatively large.

Some time ago, in an attempt to explain the low (about 2σ) rate in the Homestake experiment [3] in comparison to the LMA expectation as well as the absence of clear low energy upturn of the spectra of events at Super-Kamiokande and SNO, we have proposed a scenario with light sterile neutrino, ν_s, which mixes weakly with active neutrinos [13]. Conversion of ν_e to ν_s driven by the mass squared difference $\Delta m^2_{01} \sim (0.2\text{–}2) \times 10^{-5}$ eV^2 and mixing in the mass state ν_1, $\sin^2 2\alpha \sim 10^{-3}$, leads to appearance of a dip in the $\nu_e - \nu_e$ survival probability in the range (0.5–7) MeV which explains the data. At the same time, no statistically significant evidence of the sterile neutrino has been obtained from the global fit of the solar neutrino data in [14].[1]

After the publication [13] and analysis [14], several new experimental results have appeared which further support our proposal:

(i) Measurements of the solar neutrino spectrum by Super-Kamiokande-III [15] with lower threshold still do not show the upturn.

(ii) The SNO LETA analysis [16] gives even turn down of the spectrum in the two lowest energy bins.

(iii) The Borexino measurements of the boron neutrino spectrum also hint at some tendency of the spectral turn down [17].

Although separately these results are not statistically significant, being combined they can be considered an evidence of some new subleading effect.

At the same time, the cosmological observations indicate possible presence of additional radiation in the Universe in the epoch of last photon scattering. This is quantified by the effective number of neutrino species, $N_{\rm eff}$, which is bigger than 3. Combined analysis of WMAP-7, measurements of baryonic acoustic oscillations and new value of the Hubble constant H_0) gives $N_{\rm eff} = 4.34^{+0.86}_{-0.88}$ [18]. WMAP-7 and Atacama Cosmology Telescope data lead to $N_{\rm eff} = 5.3 \pm 1.3$ (68% C.L.) [19]. In the independent analysis [20] of these data, the number of very light sterile neutrinos $\Delta N_{\rm eff} = (0.02\text{–}2.2)$ (68% C.L.) has been obtained. All this confirms the earlier finding based on the WMAP-3 data: $N_{\rm eff} = 5.3^{+0.4+2.1+3.8}_{-0.6-1.7-2.5}$ [21].

These results do not contradict the recent big bang nucleosynthesis (BBN) bounds $N_{\rm eff} = 3.68^{+0.80}_{-0.70}$ [22] (see discussion in [23] and theoretical considerations in [24]). Hence, an additional radiation can be produced before the BBN epoch.

In this connection, we revisit our proposal of very light sterile neutrinos. We show that mixing of this neutrino in mass states ν_1 or/and ν_2 can consistently improve

[1]Although, according to Fig. 6 of [14], the bound on sterile neutrinos disappears in the range of $\Delta m^2_{01} \sim 10^{-5}$ eV^2 and $\sin^2 2\alpha < 10^{-2}$.

description of the solar spectral data. We introduce mixing of this neutrino in the mass eigenstate ν_3 which allows ν_s to be produced in the early Universe with the nearly equilibrium concentration, so that $\Delta N_{\rm eff} \approx 1$.

The paper is organized as follows. In Sec.. II, we consider properties of the ν_e conversion in the presence of ν_s-mixing in the Sun, generalizing our analysis in [13]. We further develop the formalism which allows one to understand dependence of the produced dip on the oscillation parameters. The new feature, "wiggles" in the survival probability, is described which appears for relatively large Δm^2_{01} at the $E > 5$ MeV. In Sec. III, we obtain bounds on the ν_s parameters from the Borexino measurements of the Be-neutrino flux. The spectra of the solar neutrino events have been computed for different experiments and confronted with the data. We present a simplified χ^2-fit of the spectra and find the relevant ranges of ν_s-parameters. In Sec. IV, the mixing of ν_s in ν_3 is introduced and phenomenological consequences of this mixing are studied, in particular, generation of ν_s in the early Universe. The conclusion is given in Sec. V. In Appendix A, we give some details of appearance of the wiggles in the survival probability. In Appendix B, we describe results for some alternative ν_s-mixing schemes.

II. STERILE NEUTRINO AND CONVERSION PROBABILITIES

A. Generalities

Let us consider the system of four neutrinos $\nu_f = (\nu_s, \nu_e, \nu_\mu, \nu_\tau)$ mixed in the mass eigenstates ν_i, $i = 0, 1, 2, 3$. The sterile neutrino, ν_s, is mainly present in the mass eigenstate ν_0 with mass m_0. It mixes weakly with active neutrinos, and this mixing can be treated as small perturbation of the standard LMA structure.

Coherence of all mass eigenstates is lost on the way to the Earth. Therefore, the ν_e-survival probability at the surface of the Earth can be written as

$$P_{ee} = \sum_i |A^S_{ei}|^2 |U_{ei}|^2, \tag{1}$$

where A^S_{ei} is the amplitude of $(\nu_e \to \nu_i)$ transition inside the Sun and $U_{ei} \equiv \langle \nu_e | \nu_i \rangle$ is the ei-element of the mixing matrix in vacuum. The quantities in Eq. (1) satisfy the normalization conditions: $\sum_i |U_{ei}|^2 = 1$ and

$$\sum_i |A^S_{ei}| = 1.$$

During nights, the solar neutrinos oscillate in the matter of the Earth. In this case, U_{ei} in Eq. (1) should be substituted by the $\nu_i \to \nu_e$ oscillation probabilities inside the Earth, $U_{ie} \to A^E_{ie}$, so that

$$P_{ee} = \sum_i |A^S_{ei}|^2 |A^E_{ie}|^2. \tag{2}$$

In the production point, the electron neutrino state can be represented in terms of the eigenstates in matter, ν_{im}, as

$$\nu_e = \sum_i U^m_{ei} \nu_{im}, \qquad (i = 0, 1, 2, 3),$$

where U^m_{ei} is the mixing matrix element in matter in the production region. We denote by λ_i the eigenvalues which correspond to the eigenstates ν_{im}. Introducing A_{ji}—the amplitudes of $\nu^m_i \to \nu_j$ transitions inside the Sun—we can write

$$A^S_{ei} = \sum_j U^m_{ej} A_{ji}. \tag{3}$$

Insertion of this expression into (2) gives

$$P_{ee} = \sum_i |\sum_j U^m_{ej} A_{ji}|^2 |A^E_{ie}|^2. \tag{4}$$

In the adiabatic case $A_{ij} = \delta_{ij}$, so that

$$P_{ee} = \sum_i |U^m_{ei}|^2 |A^E_{ie}|^2. \tag{5}$$

For low energies we are interested in, the Earth matter effect is small and can be neglected in the first approximation, and therefore

$$P_{ee} \approx \sum_i |\sum_j U^m_{ej} A_{ji}|^2 |U_{ei}|^2 \tag{6}$$

which we will use in our further considerations.

In what follows, we will introduce admixtures of the sterile neutrino in different mass eigenstates. In computations of effects for solar neutrinos, we neglect the 1–3 mixing and therefore consider the mixing of only three flavor states $\nu^{(3)}_f = (\nu_s, \nu_e, \nu_a)$ where ν_a is the mixture of ν_μ and ν_τ. The mixing matrix which connects these states with the mass eigenstates, $\nu_{\rm mass} = (\nu_0, \nu_1, \nu_2)$, can be parameterized as

$$U^{(3)} = U_\theta U_\alpha, \tag{7}$$

where U_α is the matrix which mixes ν_s in ν_1 or/and ν_2 and $U_\theta \equiv U_{12}(\theta_{12})$ is the standard LMA mixing (the rotation by the angle θ_{12} in the $\nu_1 - \nu_2$ plane). The Hamiltonian of the system in the $\nu^{(3)}_f$ basis can be written as

$$H_f = U^\dagger_\theta U^\dagger_\alpha H^{\rm diag} U_\alpha U_\theta + V, \tag{8}$$

where

$$H^{\rm diag} \equiv {\rm diag}(H_0, H_1, H_2) = \frac{1}{2E} {\rm diag}(m^2_0, m^2_1, m^2_2),$$
$$V \equiv {\rm diag}(0, V_e, V_a) \tag{9}$$

are the diagonal matrices of the eigenvalues of the Hamiltonian in vacuum and of the matter potentials correspondingly; $V_e = \sqrt{2} G_F (n_e - 0.5 n_n)$ and $V_a = -(1/\sqrt{2}) G_F n_n$, with n_e and n_n being the electron and neutron number densities.

It is convenient to consider effects of sterile neutrino mixing in the basis rotated by the 1–2 mixing in matter U_{θ_m}: $(\nu_s, \nu_{1m}^{\rm LMA}, \nu_{2m}^{\rm LMA})$, which would diagonalize the Hamiltonian in the absence of mixing with sterile neutrinos (i.e., when $U_\alpha = I$). In this basis, the Hamiltonian becomes

$$H_\alpha = U_{\theta_m} H_f U_{\theta_m}^\dagger = U_{\theta_m} U_\theta^\dagger U_\alpha^\dagger H^{\rm diag} U_\alpha U_\theta U_{\theta_m}^\dagger + U_{\theta_m} V U_{\theta_m}^\dagger. \quad (10)$$

Since U_α is small rotation, we can represent it as

$$U_\alpha = I + U_\delta \quad (11)$$

($U_\delta \equiv U_\alpha - I$). Inserting this expression into (10) and taking the lowest order terms in U_δ, we obtain

$$H_\alpha = H_m^{\rm diag} + H_\delta, \quad (12)$$

where

$$H_m^{\rm diag} = {\rm diag}(H_0, \lambda_1^{\rm LMA}, \lambda_2^{\rm LMA}) \quad (13)$$

is the Hamiltonian in the absence of mixing with the sterile neutrino, $\lambda_i^{\rm LMA}$ $(i = 1, 2)$ are the eigenvalues of the Hamiltonian in matter (the energy levels) in the standard 2ν-case without ν_s-mixing, and

$$H_\delta \equiv U_{\Delta\theta}^\dagger U_\delta^\dagger H^{\rm diag} U_{\Delta\theta} + {\rm h.c.} \quad (14)$$

is the correction to the Hamiltonian due to mixing with the sterile neutrino. Here, $\Delta\theta \equiv (\theta_{12} - \theta_{12}^m)$ and

$$U_{\Delta\theta} \equiv U_\theta U_{\theta_m}^\dagger = \begin{pmatrix} 1 & 0 & 0 \\ 0 & \cos(\theta_{12} - \theta_{12}^m) & -\sin(\theta_{12} - \theta_{12}^m) \\ 0 & \sin(\theta_{12} - \theta_{12}^m) & \cos(\theta_{12} - \theta_{12}^m) \end{pmatrix}. \quad (15)$$

We denote the ratio of mass squared differences as

$$R_\Delta \equiv \frac{\Delta m_{01}^2}{\Delta m_{21}^2}.$$

Depending on values of mass and mixing of the sterile neutrino, one can obtain several phenomenologically different scenarios.

B. The case $m_1 < m_0 < m_2$

This case corresponds to $R_\Delta \ll 1$, as in [13]. (Other possibilities will be considered in Appendix B.) We will first assume that ν_s mixes in ν_1 and ν_0 only, which means that the matrix U_α equals

$$U_\alpha = \begin{pmatrix} \cos\alpha & \sin\alpha & 0 \\ -\sin\alpha & \cos\alpha & 0 \\ 0 & 0 & 1 \end{pmatrix}. \quad (16)$$

For a neutrino with energy $E = 10$ MeV, the level crossing scheme is shown in Fig. 1. It gives dependence of λ_i, $(i = 0, 1, 2)$ on the distance inside the Sun (or on the density). Details of construction of this scheme can be found in [13]. For other energies, the scheme can be obtained from the one in Fig. 1 by shifting the picture with respect to the frame to the right with increase of the neutrino energy and to the left with decrease of the energy. According to Fig. 1, for $E = 10$ MeV the sterile neutrino level, λ_s, has two resonances—two crossings with the original (without ν_s) level $\lambda_1^{\rm LMA}$: at smaller density n_l^R, and at higher density, n_h^R, $(n_h^R > n_l^R)$. With increase of Δm_{01}^2 the density n_l^R increases, whereas n_h^R decreases—they approach each other and then merge.

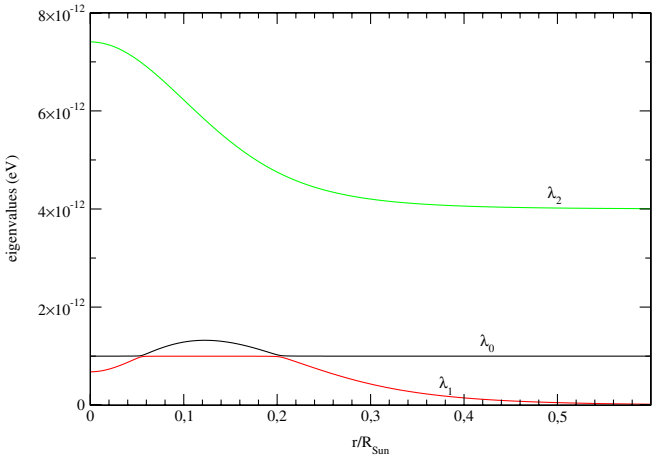

FIG. 1 (color online). The level crossing scheme for the neutrino energy $E = 10$ MeV. Dependence of the eigenvalues of the total Hamiltonian in matter, λ_i, on distance from the center of the Sun. The LMA neutrino oscillation parameters are taken as $\Delta m_{21}^2 = 8 \times 10^{-5}$ eV^2 and $\tan^2\theta_{12} = 0.44$, while the sterile neutrino parameters equal $R_\Delta = 0.25$ and $\sin^2 2\alpha = 10^{-3}$.

The flavor content of the eigenstates in matter, ν_{im}, i.e., the mixing matrix elements $U_{i\alpha}^m(n(r))$ as functions of distance from the center of the Sun is shown in Fig. 2. Since in vacuum the ν_s mixing in the ν_2 is absent, the change of

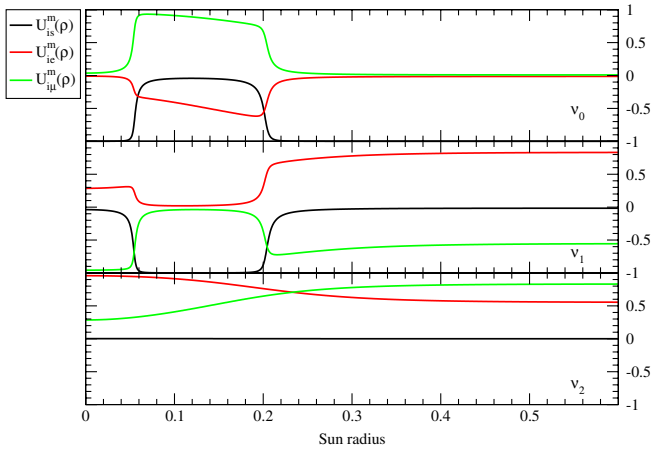

FIG. 2 (color online). Flavor content of the mass eigenstates in matter for the same values of neutrino parameters as in Fig. 1.

flavor of ν_{2m} with density ρ is approximately the same as in the LMA case: $U^m_{2\alpha}(\rho) \approx U^{m\mathrm{LMA}}_{2\alpha}(\rho)$. The intersections of the lines correspond to resonances.

Consider the evolution of this system from the production point in the central region of the Sun to the solar surface using the adiabatic basis—the basis of eigenstates ν_{im} of the instantaneous Hamiltonian. The eigenstates ν_{2m} and ν_{3m} evolve adiabatically

$$\nu_{2m} \to \nu_2, \qquad \nu_{3m} \to \nu_3,$$

i.e., $A_{2j} = \delta_{2j}$, $A_{3j} = \delta_{3j}$, and therefore according to (3)

$$A^S_{e2} = U^m_{e2}, \qquad A^S_{e3} = U^m_{e3} \approx U_{e3}. \tag{17}$$

In the last equality, we have taken into account that due to large value of Δm^2_{31} the 1–3 mixing is practically unaffected by the solar matter in the energy range of interest. Inserting the amplitudes (17) into (1), we obtain

$$P_{ee} = |A^S_{e1}|^2|U_{e1}|^2 + |A^S_{e0}|^2|U_{e0}|^2 + |U^m_{e2}|^2|U_{e2}|^2 + |U_{e3}|^4. \tag{18}$$

In turn, the amplitudes of ν_e-transitions to ν_1 and to ν_0 can be written according to (3) as

$$A^S_{e1} = U^m_{e1}A_{11} + U^m_{e0}A_{01}, \qquad A^S_{e0} = U^m_{e1}A_{10} + U^m_{e0}A_{00}. \tag{19}$$

Finally, insertion of (19) into (18) gives

$$P_{ee} = |U^m_{e1}A_{11} + U^m_{e0}A_{01}|^2|U_{e1}|^2 + |U^m_{e1}A_{10} + U^m_{e0}A_{00}|^2|U_{e0}|^2 + |U^m_{e2}|^2|U_{e2}|^2 + |U_{e3}|^4. \tag{20}$$

Since $|U_{e0}|^2 \lesssim 10^{-3}$ and $|U_{e3}|^4 \lesssim 4 \times 10^{-4}$, the probability (20) can be written approximately as

$$P_{ee} \approx |U^m_{e1}A_{11} + U^m_{e0}A_{01}|^2|U_{e1}|^2 + |U^m_{e2}|^2|U_{e2}|^2. \tag{21}$$

The survival probability in the pure LMA case is given by

$$P^{\mathrm{LMA}}_{ee} \approx |U^{m\mathrm{LMA}}_{e1}|^2|U^{\mathrm{LMA}}_{e1}|^2 + |U^{m\mathrm{LMA}}_{e2}|^2|U^{\mathrm{LMA}}_{e2}|^2 + |U_{e3}|^4. \tag{22}$$

Since ν_s mixing in the ν_2 is absent, $U^{\mathrm{LMA}}_{e2} = U_{e2}$ and $U^{m\mathrm{LMA}}_{e2} = U^m_{e2}$ and the probability (22) can be rewritten as

$$P^{\mathrm{LMA}}_{ee} \approx |U^{m\mathrm{LMA}}_{e1}|^2|U_{e1}|^2 + |U^m_{e2}|^2|U_{e2}|^2 + |U_{e3}|^4. \tag{23}$$

Let us analyze the dependence of the ν_s-mixing effect using expression (21) and the known level crossing scheme.

1. With the decrease of the neutrino energy, the pattern of Fig. 1 shifts to the left. Therefore, at low energies there are no sterile neutrino resonances, the evolution proceeds adiabatically, and

$$P_{ee} \approx |U^m_{e1}|^2|U_{e1}|^2 + |U^m_{e2}|^2|U_{e2}|^2. \tag{24}$$

Furthermore, $U^m_{e1} \approx U^{m\mathrm{LMA}}_{e1}$ and $U^m_{e2} \approx U^{m\mathrm{LMA}}_{e2}$, where $U^{m\mathrm{LMA}}_{ei}$ are mixing parameters in the pure LMA (2ν) case without sterile neutrinos. So, $P_{ee} \approx P^{\mathrm{LMA}}_{ee}$.

2. With the increase of energy, the low density resonance becomes effective (the corresponding level crossing scheme for $E = 8$ MeV is shown in Fig. 1 of our paper [13]). In the adiabatic case (relatively large U_{e0}), we have $A_{01} \approx 0$, $A_{11} \approx 1$, and the expression for P_{ee} in Eq. (21) is reduced to the one in (24). However now $U^m_{e1} \approx 0$, if the neutrino is produced above the resonance layer, and consequently, $P_{ee} \approx |U^m_{e2}|^2|U_{e2}|^2$, which differs from the usual LMA result, $P_{ee} < P^{\mathrm{LMA}}_{ee}$.

In the nonadiabatic case

$$P_{ee} \approx |U^m_{e0}A_{01}|^2|U_{e1}|^2 + |U^m_{e2}|^2|U_{e2}|^2 \approx |U^{m\mathrm{LMA}}_{e1}A_{01}|^2|U_{e1}|^2 + |U^m_{e2}|^2|U_{e2}|^2, \tag{25}$$

where we have taken into account that $U^m_{e0} \approx U^{m\mathrm{LMA}}_{e1}$. In the case of strong adiabaticity violation (for very small U_{01}) when $A_{01} \approx 1$, the probability in (25) is reduced to the standard LMA probability.

3. With the further increase of energy at $E \gtrsim 9$ MeV, the two sterile resonances are realized and the amplitudes A_{01} and A_{11} can be written in terms of the transition amplitudes in each resonance $A^{(a)}_{ij}$ ($a = 1, 2$) as

$$A_{11} = A^{(2)}_{11}A^{(1)}_{11} + A^{(2)}_{10}A^{(1)}_{01}, \qquad A_{01} = A^{(2)}_{00}A^{(1)}_{01} + A^{(2)}_{01}A^{(1)}_{11}. \tag{26}$$

One can get different results depending on the adiabaticity conditions in each resonance. If the crossings are adiabatic, $A_{01} \approx 0$, $A_{11} \approx 1$, we obtain from (21)

$$P_{ee} \approx |U^m_{e1}|^2|U_{e1}|^2 + |U^m_{e2}|^2|U_{e2}|^2.$$

This expression is similar to the one for the standard LMA case, however now $|U^m_{e1}|^2 = 1 - |U^m_{e2}|^2 - |U^m_{e0}|^2 = |U^{m\mathrm{LMA}}_{e1}|^2 - |U^m_{e0}|^2$, and consequently,

$$P_{ee} = P^{\mathrm{LMA}}_{ee} - |U_{e1}|^2|U^m_{e0}|^2.$$

Here, the second term describes the dip in the adiabatic case. Notice that due to smallness of the ν_s-mixing in vacuum one has $U_{e1} \approx U^{\mathrm{LMA}}_{e1}$. Furthermore, far above the high density resonance (in the density scale), one has $U^m_{e0} \approx 0$ and therefore $P_{ee} \approx P^{\mathrm{LMA}}_{ee}$.

If adiabaticity is strongly broken in both resonances due to smallness of sterile mixing, then $A^{(2)}_{10} \approx A^{(1)}_{01} \approx 1$ and $A^{(2)}_{11} \approx A^{(2)}_{00} \approx A^{(1)}_{11} \approx 0$. Therefore, according to (26), $A_{01} \approx 0$, $A_{11} \approx 1$, and as in the adiabatic case

$$P_{ee} \approx |U^m_{e1}|^2|U_{e1}|^2 + |U^m_{e2}|^2|U_{e2}|^2. \tag{27}$$

However, now the mixing parameters are approximately equal to the standard LMA parameters without sterile neutrinos. Therefore $P_{ee} \approx P^{\mathrm{LMA}}_{ee}$.

The flavor mixing (7) can be explicitly parameterized as

$$\nu_0 = \cos\alpha\,\nu_s + \sin\alpha(\cos\theta_{12}\nu_e - \sin\theta_{12}\nu_a),$$
$$\nu_1 = \cos\alpha(\cos\theta_{12}\nu_e - \sin\theta_{12}\nu_a) - \sin\alpha\,\nu_s,$$
$$\nu_2 = \sin\theta_{12}\nu_e + \cos\theta_{12}\nu_a.$$

Here, ν_e and ν_a (a combination of ν_μ and ν_τ) mix with the angle θ_{12} in the mass eigenstates ν_1 and ν_2 having the mass split Δm^2_{21}. In terms of these mixing angles,

$$U_{e1} = \cos\alpha\cos\theta_{12}, \quad U_{e0} = \sin\alpha\cos\theta_{12}, \quad U_{e2} = \sin\theta_{12}.$$

With this parameterization, the Eqs. (21) and (27) reproduce the corresponding results of our previous paper [13].

Further insight into dynamics of conversion can be obtained from consideration of the evolution in the rotated basis $(\nu_s, \nu^{\rm LMA}_{1m}, \nu^{\rm LMA}_{2m})$. This consideration can be used to compute the amplitudes A_{ij}. From Eqs. (12)–(15), we find using (16) that the Hamiltonian in the rotated basis equals

$$H_\alpha = \begin{pmatrix} 0 & -\frac{\Delta m^2_{01}}{2E}\sin\alpha\cos(\theta_{12}-\theta^m_{12}) & -\frac{\Delta m^2_{01}}{2E}\sin\alpha\sin(\theta_{12}-\theta^m_{12}) \\ \dots & \lambda^{\rm LMA}_1 - H_0 & 0 \\ \dots & \dots & \lambda^{\rm LMA}_2 - H_0 \end{pmatrix}. \tag{28}$$

Because of smallness of α, the off-diagonal terms are much smaller than the diagonal ones. If $R_\Delta \ll 1$, so that $H_0 \equiv m^2_0/2E$ is close to $\lambda^{\rm LMA}_1$ and crosses this level. In this case, there is no crossing of $\lambda^{\rm LMA}_2$ and H_0 levels, the 1–3 element of matrix (28) can be neglected so that the state $\nu^{\rm LMA}_{2m}$ decouples. Then mixing of ν_s and $\nu^{\rm LMA}_{1m}$ is determined by the 1–2 element of (28):

$$\sin\alpha\frac{\Delta m^2_{01}}{2E}\cos(\theta_{12}-\theta^m_{12}) = \sin\alpha\frac{\Delta m^2_{21}}{2E}R_\Delta\cos(\theta_{12}-\theta^m_{12}). \tag{29}$$

Since the transition occurs in the resonance region, θ_m should be taken at the density which corresponds to the sterile neutrino resonance. The expression for mixing (29) allows one to understand behavior of the conversion probability on R_Δ, α, and neutrino energy.

C. Dip and wiggles

In Figs. 3 and 4, we show the results of numerical computations of the ν_e survival probability P_{ee} as functions of the neutrino energy. We have performed complete integration of the evolution equations for the 3ν-system and also made averaging over the neutrino production region in the Sun.

The ν_s-mixing and $\nu_e \to \nu_s$ conversion lead to appearance of a dip in the energy dependence of the ν_e- survival probability. Using normalization conditions

$$|A^S_{e1}|^2 + |A^S_{e0}|^2 + |U^m_{e2}|^2 = 1$$

(we neglect the 1–3 mixing here) and $\sum_i |U_{ei}|^2 = 1$ ($i = 0$, 1, 2, 3) as well as the expressions in Eqs. (18) and (23) we find the difference of probabilities with and without sterile neutrino effect:

$$\Delta P_{ee} \equiv P^{\rm LMA}_{ee} - P_{ee}$$
$$= |A^S_{e0}|^2(1-|U_{e2}|^2) - |U_{e0}|^2(2|A^S_{e0}|^2 - 1 - |U^m_{e2}|^2)$$
$$\approx |A^S_{e0}|^2(1-|U_{e2}|^2) \approx P_{es}(1-|U_{e2}|^2),$$

where $P_{es} \approx |A^S_{e0}|^2$ is the probability of $\nu_e \to \nu_s$ transition. The quantity ΔP_{ee} describes the dip which has the following properties (see Fig. 3 and also discussion in [13]):

(1) A position of the dip (its low energy edge) is given by the low density resonance taken at the central density of the Sun $E_l(n_c)$. With the increase of Δm^2_{01}, the dip shifts to higher energies.

(2) Maximal suppression in the dip depends on R_Δ and α. For small R_Δ (large distance between the two ν_s-resonances) and large α ($\sin^2 2\alpha > 10^{-3}$), the absolute minimum can be achieved at the adiabatic crossing of the ν_s-resonances. With increase of R_Δ (decrease of distance between the resonances) and/or decrease of α (stronger violation of the adiabaticity) a suppression in the dip weakens. Also with decrease of α the dip becomes narrower.

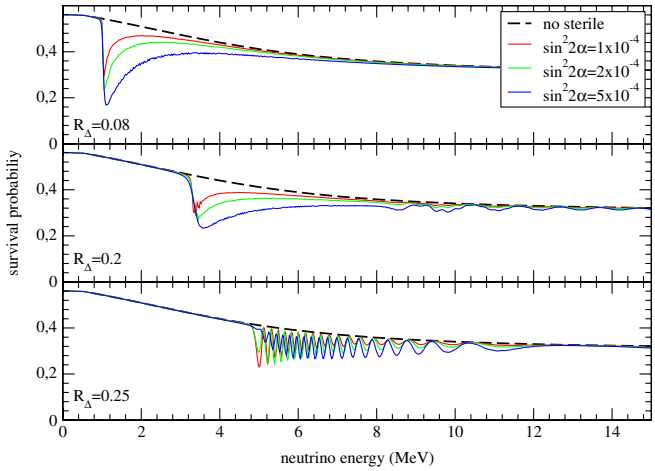

FIG. 3 (color online). The survival probability of the electron neutrino as a function of neutrino energy for different values of the sterile-active mixing parameter $\sin^2 2\alpha$ and mass scale $R_\Delta \ll 1$. The active neutrino parameters are $\Delta m^2_{21} = 8\times 10^{-5}$ eV^2 and $\tan^2\theta_{12} = 0.44$.

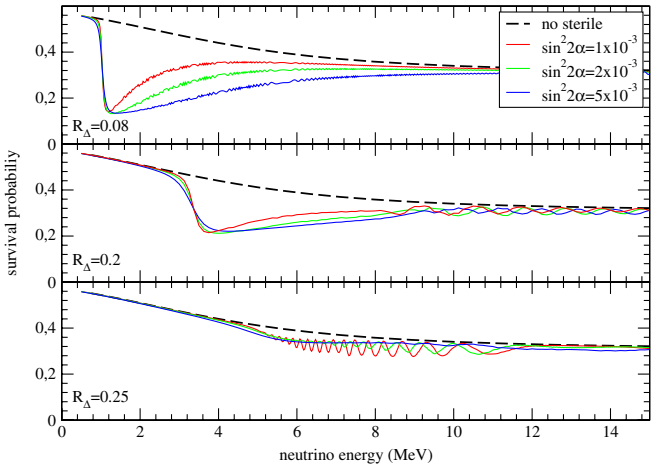

FIG. 4 (color online). The same as in Fig. 3 for higher values of mixing angle α.

(3) For large Δm^2_{01} and relatively small α, the survival probability as function of the neutrino energy has wiggles (see Fig. 3). The wiggles are a result of the interference of the two amplitudes in the first term of (21) which develops over finite space interval. Indeed, according to (21), there are two channels of transition of ν_e to ν_1:

(i) ν_e has admixture U^m_{e1} in ν_{1m}, the latter adiabatically evolves to ν_1: $\nu_e \to \nu_{1m} \to \nu_1$, and the amplitude equals $U^m_{e1}A_{11}$.

(ii) ν_e has admixture U^m_{e0} in ν_{0m}; this state transforms to ν_1 due to nonadiabatic transition: $\nu_e \to \nu_{0m} \to \nu_1$. The corresponding amplitude is $U^m_{e0}A_{01}$.

The two contributions to the amplitude interfere leading to the oscillatory dependence of the probability on energy (wiggles). Introducing $P_{01} \equiv |A_{01}|^2$, so that $|A_{11}|^2 = 1 - P_{01}$, we can rewrite the probability (21) as

$$P_{ee} \approx |U_{e1}|^2[|U^m_{e1}|^2(1 - P_{01}) + |U^m_{e0}|^2 P_{01} + U^m_{e1}U^m_{e0}\cos\phi\sqrt{P_{01}(1 - P_{01})}] + |U_{e2}|^2|U^m_{e2}|^2,$$

where $\phi \equiv \arg(A^*_{01}A_{11})$ and we assumed for simplicity that U^m_{e1} and U^m_{e0} are real. The oscillatory behavior follows from the energy dependence of the phase ϕ. The key point is that the phase is collected over restricted space interval, L, and therefore is not averaged out even after integration over the production region. Indeed, the phase ϕ is acquired from the neutrino production point to the second (low density) resonance. Below the second resonance (in density) both "trajectories" (channels of transition) coincide. Appearance of the wiggles requires the adiabaticity violation. In the adiabatic case, $A_{01} = 0$, only one channel exists. Unfortunately, it will be difficult, if possible, to observe experimentally these wiggles. Some more details concerning the wiggles are presented in Appendix A.

If ν_s mixes in ν_2, then

$$U_\alpha = \begin{pmatrix} \cos\alpha' & 0 & \sin\alpha' \\ 0 & 1 & 0 \\ -\sin\alpha' & 0 & \cos\alpha' \end{pmatrix} \quad (30)$$

and the Hamiltonian can be obtained from (28) by substitutions

$$\cos(\theta_{12} - \theta^m_{12}) \to \sin(\theta_{12} - \theta^m_{12}),$$
$$\sin(\theta_{12} - \theta^m_{12}) \to -\cos(\theta_{12} - \theta^m_{12}), \quad (31)$$
$$\Delta m^2_{01} \to \Delta m^2_{02}.$$

The state ν_{2m} decouples and the $\nu_s - \nu^{\rm LMA}_{1m}$ mixing is given by

$$\sin\alpha' \frac{\Delta m^2_{02}}{2E}\sin(\theta_{12} - \theta^m_{12}) = \sin\alpha' \frac{\Delta m^2_{21}}{2E}(1 - R_\Delta)\sin(\theta_{12} - \theta^m_{12}). \quad (32)$$

Notice that this mixing appears due to the matter effect and it is absent in vacuum when $\theta^m_{12} \to \theta_{12}$. It happens that for values of R_Δ we are considering $(1 - R_\Delta) \times \sin(\theta_{12} - \theta^m_{12}) \approx R_\Delta \cos(\theta_{12} - \theta^m_{12})$, and therefore the probabilities in this case are very similar to those shown in Figs. 3 and 4.

III. SOLAR NEUTRINO DATA AND STERILE NEUTRINO EFFECT

In what follows, we will consider scenario with $m_1 < m_0 < m_2$. This possibility gives better description of the data: it leads to significant modification of the survival probability in the transition region and weakly affects spectra at high energies.

A. Borexino measurements of the Be-neutrino line

The results of Borexino experiment [10] are in a very good agreement with prediction based on the LMA solution and thestandard solar model. Within the error bars, no additional suppression of the flux has been found on the top of $P^{\rm LMA}_{ee}$. In Borexino (and other experiments based on the νe-scattering), the ratio of the numbers of events with and without conversion can be written as

$$R_{\rm Borexino} = P_{ee}(1 - r) + r - rP_{es}, \quad (33)$$

where $r \equiv \sigma(\nu_\mu e - \nu_\mu e)/\sigma(\nu_e e - \nu_e e)$ is the ratio of cross sections. Using Eq. (33), we find an additional suppression of the Borexino rate in comparison with the pure LMA case [13]:

$$\Delta R_{\rm Borexino} \equiv R^{\rm LMA}_{\rm Borexino} - R_{\rm Borexino} = (1 - r)\Delta P_{ee} + rP_{es} \approx \Delta P_{ee}(1 + r\tan^2\theta_{12}).$$

In Fig. 5, we show dependence of the survival probability at $E = E_{Be}$ as a function of R_Δ for two different values of

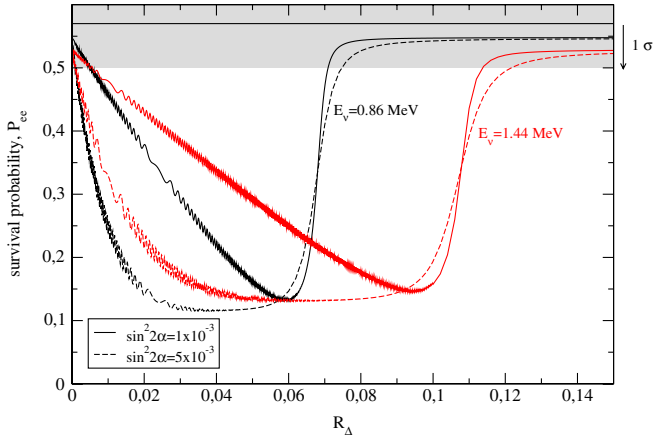

FIG. 5 (color online). The survival probabilities for the monoenergetic ^{7}Be- ($E_\nu = 0.86$ MeV) and *pep*- ($E_\nu = 1.44$ MeV) neutrino fluxes as functions of R_Δ, for two values of mixing: $\sin^2 2\alpha = 1 \times 10^{-3}$ (solid lines) and 5×10^{-3} (dashed lines). The active neutrino oscillation parameters are the same as in Fig. 3. The horizontal line and shadowed band show, respectively, the central value and 1σ band for the suppression factor determined by Borexino.

the mixing angle α. We show the Borexino bounds on P_{ee} obtained from the experimental result [17] and relation (33). According to this figure for $\sin^2 2\alpha = 10^{-3}$, the range $R_\Delta = 0.005 - 0.072$ is excluded at 1σ level. For $\sin^2 2\alpha = 5 \times 10^{-3}$, we obtain a slightly larger exclusion interval: $R_\Delta = 0.001$–0.075. The Be-neutrino line can not be in the dip, or the dip should be shallow, which then will have little impact on the higher energy spectrum. So, essentially the allowed values of masses (which influence the upturn) are

$$R_\Delta \geq 0.075, \quad \text{or} \quad \Delta m^2_{01} \geq 0.5\text{–}10^{-5}\ \text{eV}^2.$$

B. Upturn of the boron neutrino spectrum

Using the survival probabilities obtained in Sec. II, we have computed the energy spectra of events for different experiments with and without sterile neutrino. These spectra together with experimental data are presented in Figs. 6–10. Notice that due to uncertainty in the original boron neutrino flux, the experimental points can be shifted with respect to the theoretical lines by about 15%.

In Figs. 6 and 7, we show the ratio of the number of events in Super-Kamiokande-I (SK-I) with and without oscillations for two different values of R_Δ. Different curves correspond to the standard LMA solution (dashed) and the spectra with conversion to sterile neutrino. In the presence of sterile neutrino mixing the upturn can be completely eliminated and even transformed into turn down of the spectrum. In Fig. 6 the dip at $E \sim 4$ MeV corresponds to the dip in the probability at approximately the same energy as in the Fig. 3 (middle panel). The difference of the predictions with and without sterile neutrino can be as big as (15–20)% at $E_e < 5$ MeV.

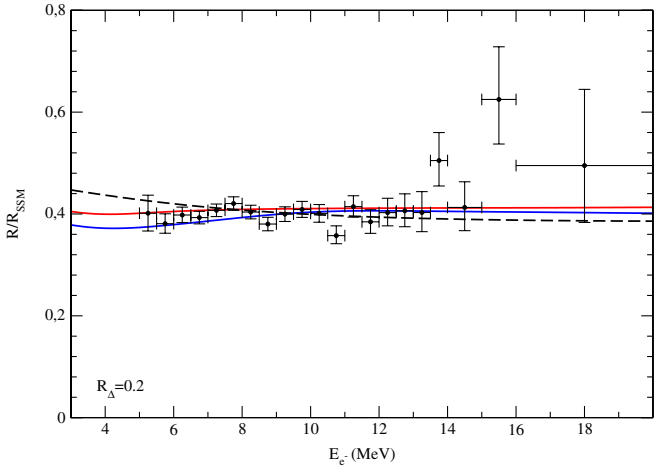

FIG. 6 (color online). The predicted Super-Kamiokande-I energy spectrum versus the experimental data [6]. The active neutrino parameters are the same as before; the sterile neutrino parameters equal $R_\Delta = 0.20$ and $\sin^2 2\alpha = 1 \times 10^{-3}$ (red line, weaker upturn suppression) and 5×10^{-3} (blue line, stronger upturn suppression). The pure LMA spectrum is presented by the dashed black line, with a normalization factor $f_B = 0.91$ to reproduce the total observed number of events. We use the ^{8}B-neutrino flux according to the GS98 solar model [25].

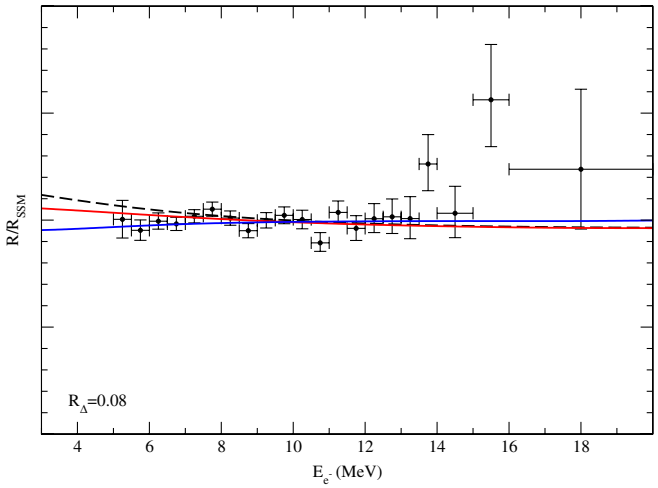

FIG. 7 (color online). The same as in Fig. 6, but for $R_\Delta = 0.08$.

The SuperKamiokande-III data (SK-III) (Fig. 8) has the additional lower energy bin [15], however statistics are lower than in SK-I. Again, there is no clear indication of the upturn in the SK-III spectrum and theoretical lines with sterile neutrino mixing can describe the data better than pure LMA solution.

SNO (Fig. 9) is more sensitive to distortion of the neutrino spectrum. However, the dip in the electron energy spectrum is shifted to low energies by the threshold of the CC reaction on the deuteron: $E = 1.44$ MeV. Experimental points are from the SNO-LETA charge current event analysis [16]. Two low energy points of the spectrum show a sharp turn down. This can not be

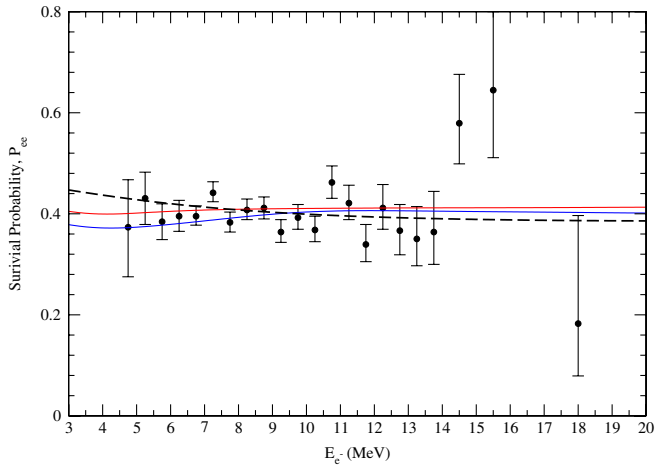

FIG. 8 (color online). The predicted Super-Kamiokande-III energy spectrum versus the experimental data [15]. The neutrino parameters and the solar model as well as the normalization factor for pure LMA spectrum are the same as in Fig. 6 (left).

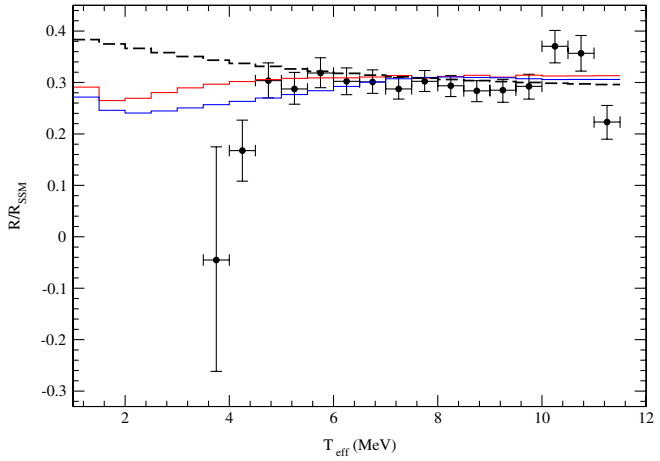

FIG. 9 (color online). Prediction for the SNO-LETA electron spectrum versus experimental data [16]. The neutrino parameters and the solar model are the same as in Fig. 6.

reproduced by the proposed dip, although with the dip the description is better.[2] Also, the Borexino spectrum (Fig. 10) can be fitted better in the presence of sterile neutrino mixing.

C. Fit of spectra

As follows from Figs. 6–10, the mixing with sterile neutrino improves description of the data. It is also clear that, with the present data, it is not possible to make a conclusion about existence of ν_s-mixing. Further experimental studies of the solar neutrino spectrum in the intermediate energy range are needed. In view of this for

[2]Too sharp a decrease of signal in the lowest energy bins is probably statistical fluctuations or some systematics.

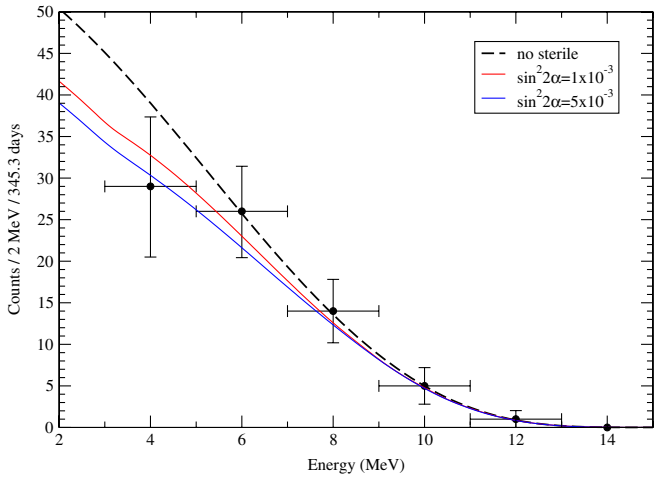

FIG. 10 (color online). The predicted energy spectrum of events due to the ^{8}B-neutrinos at Borexino versus the experimental data [17]. The neutrino parameters and the solar model are the same as in Fig. 6.

illustrative purposes, we have performed a simplified χ^2-fit of the energy spectra shown in Figs. 6–10. This will allow us to quantify somehow the improvement of the description and to determine plausible values of parameters of ν_s.

For the best fit values of ν_s parameters, we have the following improvements in individual experiments: $\Delta\chi^2 = 1.94$ (SK-I), 0.81 (SK-III), 3.52 (SNO), 0.63 (Borexino) 0.56 (SNO-NC), 7.45 (Total).

In our χ^2 analysis, we use the spectra from SK-I (21 data points), SK-III (21 points), SNO-LETA (16 points), Borexino (6 points), and SNO-LETA neutral current result (1 point)—altogether 65 degrees of freedom. Recall that all these experiments are sensitive to the same ^{8}B-neutrino flux. We use α and Δm^2_{01} as the fit parameters and fix θ_{12} and Δm^2_{21} to their best fit values from the 2ν- LMA analysis. Since oscillations to sterile neutrinos change the neutral current event rate, we cannot use the SNO-LETA neutral currentresult to fix the boron neutrino flux in the model independent way. Therefore, we have performed fit of the spectra employing two different procedures.

In the first approach, we use the boron neutrino flux predicted in the solar neutrino model GS98 [25]: $F_B^{\rm SSM} = 5.88 \times 10^{-6}$ cm^{-2} s^{-1}. We computed the difference of χ^2 obtained in the fits without sterile neutrinos χ^2 and with sterile neutrinos χ^2_s: $\Delta\chi^2 \equiv \chi^2 - \chi^2_s$ (see Table I). We find that the strongest improvement, $\Delta\chi^2 = 7.5$, is obtained for

$$\Delta m^2_{01} \approx 1.6 \times 10^{-5}\ \text{eV}^2, \qquad \sin^2 2\alpha \approx 10^{-3}.$$

For 65 degrees of freedom and two fit parameters, this $\Delta\chi^2$ corresponds to an increase of goodness of the fit from 16% to 25%. The fit with $\Delta\chi^2 > 6$ can be obtained in the range

$$R_\Delta = 0.12\text{–}0.22, \qquad \sin^2 2\alpha = (0.6\text{–}1.3) \times 10^{-3}. \quad (34)$$

The range of R_Δ in (34) corresponds to $\Delta m^2_{01} \sim (0.9\text{–}1.8) \times 10^{-5}$ eV^2 and therefore

TABLE I. Results of the χ^2-fit of the solar neutrino spectra. Shown are values of $\Delta\chi^2$ (see text) for different values of $\sin^2 2\alpha$ and R_Δ.

$\sin^2 2\alpha / R_\Delta$:	0.08	0.20	0.25	1.10	1.30	1.50
0.0001	0.62	1.70	4.89	1.40	4.12	1.12
0.0002	0.96	3.00	5.26	2.58	5.88	−3.82
0.0005	1.69	6.04	5.93	5.20	0.11	−44.5
0.001	2.79	7.45	5.74	6.61	−38.8	−194
0.002	4.36	4.84	4.27	−1.18	−206	−694
0.005	5.41	−2.99	4.23	−109	−1121	−1795

$$m_0 \geq (3\text{–}4) \times 10^{-3}\ \text{eV}. \tag{35}$$

In the second approach, we use the boron neutrino flux as a free parameter introducing $f_B \equiv F_B / F_B^{\rm SSM}$. In this case, the improvement of the fit with sterile neutrino is much weaker: $\Delta\chi^2 = 2.5$, and the goodness of the fit is practically the same, 26%, with and without the ν_s-mixing. We obtain here the normalization factor with respect to the GS98 model prediction $f_B \approx 0.95$ in the presence of a sterile neutrino, and $f_B \approx 0.86$ without ν_s. This indicates that mixing with ν_s leads to better agreement with prediction of the GS98 model.

The statistical significance is recovered if θ_{12} and Δm^2_{21} are also included in the fit. In this case, however, one needs to perform the global fit of all the solar neutrino data.

In the case $R_\Delta > 1$, only a small region of parameters near $R_\Delta \sim 1.1$ and $\sin^2\alpha = (0.5\text{–}1) \times 10^{-3}$ give an improvement with $\Delta\chi^2 \sim 6$.

Recall that suppression of the ν_e-fluxes in the intermediate energy range also suppresses the predicted Argon production rate [13], thus improving agreement with the Homestake result.

D. Further tests

With higher statistics, Borexino will improve precision of measurements of the boron neutrino spectrum. Also, SuperKamiokande will achieve better measurements of spectrum at lower energies. The KamLAND solar [26] and SNO$^+$ [27] experiments will further check the presence of the dip.

Additional probes of the existence of sterile neutrino (and restriction on its parameters) can be provided by measurements of the *pep*-neutrino line with $E = 1.44$ MeV since the *pep*-neutrino flux is known with high precision. In Fig. 5, we show dependence of the suppression factor for the *pep*-neutrinos as function of R_Δ. With increase of R_Δ the dip shifts to higher energies. In the interval $R_\Delta = 0.07\text{–}0.11$, the Be-neutrino flux has the LMA suppression, whereas the *pep*-flux can be suppressed by factor 0.15–0.20 (the LMA suppression is 0.52). In the range $R_\Delta > 0.12$, both the fluxes have the LMA suppression.

In the range $R_\Delta > 0.12$, the CNO-neutrino fluxes should be strongly affected by the presence of the dip. However, it will be difficult to disentangle this suppression since the original fluxes of these neutrinos are not well known.

IV. EXTRA RADIATION IN THE UNIVERSE AND $\nu_s - \nu_3$ MIXING

The smallness of mixing of the sterile neutrino in the states ν_1 or/and ν_2 ($|U_{si}|^2 < 10^{-3}$) does not lead to significant production of ν_s in the early Universe via neutrino oscillations [13]. However, high (up to the equilibrium one) concentration of ν_s can be generated if ν_s mixes in the state ν_3 and U_{s3} is large enough. Description of the solar neutrino data presented in the previous sections does not change substantially, if ν_s mixes with the combination

$$\nu'_\tau \equiv \cos\theta_{23}\nu_\tau + \sin\theta_{23}\nu_\mu \approx \nu_3,$$

where θ_{23} is the standard 2–3 mixing angle. The $\nu_s - \nu'_\tau$ mixing can be parametrized by the angle β as

$$\nu_3 \approx \cos\beta\nu'_\tau + \sin\beta\nu_s, \qquad \nu_0 \approx \cos\beta\nu_s - \sin\beta\nu'_\tau, \tag{36}$$

so that $U_{s3} \approx \sin\beta$. Here we neglect small rotations by the angles α and θ_{13} which do not influence conclusions of this section. (These mixings can be introduced before or after the rotation (36)). Since $\Delta m^2_{01} \ll \Delta m^2_{21} \ll \Delta m^2_{31}$, the mass squared difference of ν_3 and ν_0 equals

$$\Delta m^2_{30} \approx \Delta m^2_{31} = 2.4 \times 10^{-3}\ \text{eV}^2.$$

For this value of Δm^2_{30}, the mixing angle β is restricted by the atmospheric neutrino data [14]:

$$\sin^2\beta \leq 0.2\text{–}0.3, \qquad (90\%\ \text{C.L.})$$

and by the MINOS searches for depletion of the neutral current events [28]. For zero 1–3 mixing, the bound $\beta < 26^\circ$ has been established [28] which corresponds to

$$\sin^2\beta \leq 0.2, \qquad (90\%\ \text{C.L.}).$$

In the presence of nonzero 1–3 mixing, the bound becomes much weaker.

If $\sin^2\beta \sim 0.2$, then according to [29] the sterile neutrinos practically equilibrate before the BBN epoch both in the resonance channel and in nonresonance channels, i.e. in neutrino and antineutrino channels. Consequently, in the epoch of nucleosynthesis and latter, the additional effective number of neutrinos is

$$\Delta N_{\rm eff} \approx 1.$$

The value $\Delta N_{\rm eff} \approx 0.8$ can be obtained for $\sin^2\beta \approx 0.03$ in the nonresonance channel and $\sin^2\beta \sim 10^{-3}$ in the resonance channel. According to [14] $\Delta N_{\rm eff} \approx 0.8$ is generated, if the $\nu_s - \nu_\mu$ mixing is about $\sin^2\beta = 0.02$.

The CNGS experiment has also some potential to restrict $\sin^2\beta$ [30].

Let us consider other phenomenological consequences of the $\nu'_\tau - \nu_s$ mixing. The level crossing scheme can be

obtained from Fig. 1 by adding the third active neutrino level and expanding the whole picture to the left. With increase of density, the value of λ_2 increases until the 1–3 resonance density and then turns down and decreases in parallel to λ_1. Consequently, the sterile level $\lambda_s \approx \lambda_0$ (horizontal line) will cross λ_2 at some density above the 1–3 resonance density. Thus, the mixing of ν_s in ν_3 leads to appearance of the resonance in $\nu'_\tau - \nu_s$ channel (normal mass hierarchy) at the density determined by

$$V_a = \frac{1}{\sqrt{2}} G_F n_n \approx \frac{\Delta m^2_{03}}{2E} \approx \frac{\Delta m^2_{31}}{2E}.$$

In the isotopically neutral medium, this density is about two times larger than the density of 1–3 resonance. For the inverted mass hierarchy, the resonance appears in the antineutrino channel $\bar{\nu}'_\tau - \bar{\nu}_s$.

Inside the Earth, the $\nu'_\tau - \nu_s$ resonance energy equals $E \approx 12$ GeV and a wide resonance dip in the ν_μ survival probability should appear in the range (10–15) GeV. This can be tested in studies of the atmospheric neutrinos (spectra, zenith angle dependences) in the IceCube DeepCore detector [31] and in next generation Megaton-scale experiments [32]. The effect of such a mixing should show up in the long baseline experiments as the energy dependent disappearance of the ν_μ-flux.

The $\nu'_\tau - \nu_s$ mixing also influences the supernova neutrino conversion. The corresponding level crossing in the collapsing star will be adiabatic (at least before the shock wave arrival), and therefore ν'_τ converts almost completely in this resonance into ν_s. At larger distances from the center of a star, this ν_s-flux will encounter the lower density ν_s resonances due to the ν_s and ν_{1m} levels crossing (see Fig. 1). The latter will lead to partial conversion of ν_s into ν_e, since the adiabaticity is broken in these resonances. Hence, the following chain of transitions is realized:

$$\nu'_\tau(\nu_\mu, \nu_\tau) \rightarrow \nu_s \rightarrow \nu_s, \nu_e, \nu'_\mu. \tag{37}$$

That would lead to partial convertion of the ν_μ and $\nu_t au$ fluxes in to ν_s flux. In the adiabatic or strongly nonadiabatic cases, ν'_τ converts in ν_s completely. In the case of inverted mass hierarchy similar consideration holds for the antineutrino channels.

In this consideration for simplicity we have neglected possible collective effects due to neutrino-neutrino scattering and effects of shock wave propagation (see [32]).

V. CONCLUSIONS

1. The recent measurements of the energy spectra of the solar neutrino events at SuperKamiokande, SNO, and Borexino do not show the expected (according to LMA) upturns of the spectra at low energies. The absence of the upturns can be explained by mixing of very light sterile neutrino in the mass states ν_1 or/and ν_2 with $\Delta m^2_{01} \sim (0.7\text{–}2) \times 10^{-5}$ eV^2 $(R_\Delta = 0.07\text{–}0.25)$ and mixing $\sin^2 2\alpha = (1\text{–}5) \times 10^{-3}$. Such a mixing leads to the appearance of a dip in the ν_e- survival probability in the energy range (1–7) MeV, thus removing the upturn of the spectra. For $\Delta m^2_{01} \sim 2 \times 10^{-5}$ eV^2 and $\sin^2 2\alpha \sim 5 \times 10^{-3}$, the $\nu_e - \nu_s$ conversion can even produce a turn down of the spectra. Description of the existing solar neutrino data in the presence of mixing with sterile neutrino is improved.

2. We generalized an analytic consideration in [13] showing that the conversion in the 4ν-mixing scheme with two different matter potentials is reduced to 2ν-conversion with density-dependent mixing. New features which appear here include (i) existence two sterile resonances—two crossings of the ν_s and $\nu^{\rm LMA}_{1m}$ levels, (ii) the mixing induced by matter effect, (iii) the interference over finite spatial interval which leads to wiggles in the energy dependence of the survival probability.

3. For the mixing angle interval $\sin^2 2\alpha = (0.5\text{–}5) \times 10^{-3}$ the values of $\Delta m^2 < 0.6 \times 10^{-5}$ eV^2 are excluded by the Borexino measurements of the Be-neutrino flux. The best fit of the spectra can be obtained for $\Delta m^2_{01} \sim 1.6 \times 10^{-5}$ eV^2 and $\sin^2 2\alpha = (0.8\text{–}1.0) \times 10^{-3}$. The presence of the dip can be tested in future precision measurements of the low energy part of the ^{8}B-neutrino spectrum as well as of the *pep*-neutrino flux.

4. The mixing of ν_s in the ν_3 mass eigenstate with $|U_{s3}|^2 \sim 0.02\text{–}0.2$ leads to production of significant concentration of ν_s via oscillations in the early Universe. For $|U_{s3}|^2 \sim 0.1 - 0.2$, the nearly equilibrium concentration can be obtained both in the neutrino and antineutrino channels, thus generating an effective number of neutrinos $\Delta N_{\rm eff} \sim 1$ before the BBN epoch. This can explain the recent cosmological observations.

5. The mixing of ν_s in ν_3 leads to a number of phenomenological consequences, in particular, it can affect the atmospheric and accelerators neutrino fluxes as well as fluxes of the supernova neutrinos. The mixing leads to existence of the $\nu_s - \nu'_\tau$ resonance. For neutrinos crossing the Earth the resonance is realized at energies $E \sim (10\text{–}15)$ GeV. This can be tested in the DeepCore IceCube experiment and future atmospheric neutrino studies with Megaton-scale detectors, as well as in long baseline experiments with accelerator neutrino beams.

ACKNOWLEDGMENTS

P. C. de Holanda is grateful to the AS ICTP for hospitality during his visit where most parts of this paper have been accomplished.

APPENDIX A: WIGGLES

As we described in Sec. II, the wiggles in dependence of the ν_e-survival probability on energy are the result of interference of the amplitudes which contribute to the

same, $\nu_e \to \nu_1$, transition. The zoomed view of the survival, P_{ee}, and transition, P_{es}, probabilities is shown in Fig. 11. The period of wiggles is about (0.5–0.6) MeV.

The key feature which leads to the wiggles with rather large period in the energy scale, and therefore prevents them from being averaged out at integration over the neutrino production region, is that the interference phase is collected over relatively small distances L. These are the distances between the production point and the low density ν_s-resonance, or the distance between the two ν_s resonances as can be seen in the Fig. 12. For the neutrino energy $E \sim 8$ MeV, the interval of the wiggles formation equals $L \approx 20 l_m$ where l_m is the oscillation length in matter. Therefore, the period of wiggles can be estimated as $\Delta E/E \sim l_m/L \sim 1/20$ in agreement with results of Fig. 12.

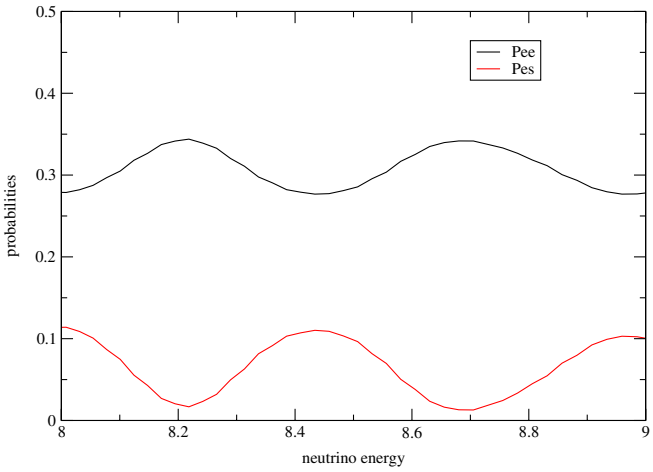

FIG. 11 (color online). A zoomed view of the survival and transition probabilities in the neutrino energy range where the wiggles can be well seen. The sterile neutrino parameters equal $R_\Delta = 0.25$ and $\sin^2 2\alpha = 10^{-3}$.

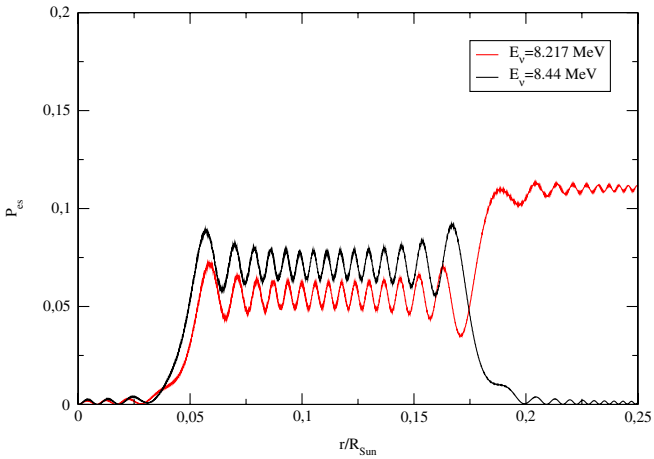

FIG. 12 (color online). The $\nu_e \to \nu_s$-transition probability for neutrinos created in the solar center as function of distance from the center of the Sun. The sterile neutrino parameters equal $R_\Delta = 0.25$ and $\sin^2 2\alpha = 10^{-3}$.

The wiggles are partially averaged due to integration over the production region. Notice that with decrease of Δm^2_{01} the lower resonance shifts to lower densities and the distance L increases leading to smaller period of wiggles and stronger averaging. This is one of the reasons of disappearance of wiggles with decrease of Δm^2_{01}. The amplitude of wiggles also decreases with the increase of α: the latter means better adiabaticity and therefore suppression of the contribution of one of the channels responsible for interference.

APPENDIX B: THE CASE $m_0 > m_2 > m_1$ AND OTHER POSSIBILITIES

For $m_0 > m_2 > m_1$ the ratio $R_\Delta > 1$. Since below the LMA resonance the eigenvalue $\lambda_2 = \lambda_2^{\rm LMA}$ and the potential V_a have practically the same dependences on density (radius) (see Fig. 1), there is only one crossing of λ_s with $\lambda_2^{\rm LMA}$, and there are no crossings for $\Delta m^2_{02} < 0$. Now the evolution of states ν_{1m} and ν_{3m} is adiabatic, so that

$$A^S_{e1} \approx U^m_{e1} = U^{m\rm LMA}_{e1}, \qquad A^S_{e3} \approx U_{e3}.$$

Consequently,

$$P_{ee} = |U^m_{e1}|^2|U_{e1}|^2 + |A^S_{e2}|^2|U_{e2}|^2 + |A^S_{e0}|^2|U_{e0}|^2 + |U_{e3}|^4,$$

where

$$A^S_{e2} = U^m_{e2}A_{22} + U^m_{e0}A_{02}, \qquad A^S_{e0} = U^m_{e2}A_{20} + U^m_{e0}A_{00}.$$

These expressions are similar to the expressions in (18) and (3) with interchange of indexes $1 \leftrightarrow 2$.

In the adiabatic case, we have

$$P_{ee} = |U^m_{e1}|^2|U_{e1}|^2 + |U^m_{e2}|^2|U_{e2}|^2 + |U^m_{e0}|^2|U_{e0}|^2 + |U_{e3}|^4.$$

Now, the effect of sterile neutrino is due to the difference of U^m_{e2} and $U^{m\rm LMA}_{e2}$: $|U^m_{e2}|^2 = |U^{m\rm LMA}_{e2}|^2 - |U^m_{e0}|^2$. In the strongly nonadiabatic case, one has $A_{20} \approx A_{02} \approx 1$, and consequently,

$$P_{ee} = |U^m_{e1}|^2|U_{e1}|^2 + |U^m_{e2}|^2|U_{e0}|^2 + |U^m_{e0}|^2|U_{e2}|^2 + |U_{e3}|^4, \tag{38}$$

with $U^m_{e2} \approx 0$, and $U^m_{e0} \approx U^{m\rm LMA}_{e2}$, so that (38) is reduced to the LMA probability.

For the ν_s-mixing in ν_0 and ν_1, the Hamiltonian is given by the same expression as in Eq. (28). However, now H_0 crosses $\lambda_2^{\rm LMA}$ and the state $\nu^{\rm LMA}_{1m}$ decouples. According to (28), the mixing of ν_s and $\nu^{\rm LMA}_{2m}$ is determined by

$$\sin\alpha \frac{\Delta m^2_{01}}{2E} \sin(\theta_{12} - \theta^m_{12}) = \sin\alpha \frac{\Delta m^2_{21}}{2E} R_\Delta \sin(\theta_{12} - \theta^m_{12}), \tag{39}$$

and this mixing is due to matter effect. In the case of ν_s-mixing in ν_0 and ν_2, performing substitutions (31) we obtain the $\nu_s - \nu_{2m}^{\rm LMA}$ mixing element

$$\sin\alpha' \frac{\Delta m_{02}^2}{2E} \cos(\theta_{12} - \theta_{12}^m) = \sin\alpha' \frac{\Delta m_{21}^2}{2E}(1 - R_\Delta)\cos(\theta_{12} - \theta_{12}^m). \quad (40)$$

In Eq. (39), the mixing being proportional to $R_\Delta \sin(\theta_{12} - \theta_{12}^m)$ is larger than in the second case (40): $\propto (1 - R_\Delta) \times \cos(\theta_{12} - \theta_{12}^m)$, since $R_\Delta \sim 1$. Furthermore, the mixing in (39) increases with energy: the sterile resonance is above the LMA resonance and therefore $\theta_{12}^m > 45°$; this angle, and consequently $|\sin(\theta_{12} - \theta_{12}^m)|$, increase. As a result, the effect does not disappear at high energies (see Figs. 13 and 14). In general, this makes the fit worthier than in the case described in the text.

In comparison to the case $R_\Delta \ll 1$, now ν_e has smaller admixture in ν_2, $|U_{e2}| < |U_{e1}|$, however the initial admixture of ν_e in ν_{2m} can be larger: $|U_{e2}^m| > |U_{e1}^m|$. Therefore, the overall effect is large (see Figs. 13 and 14). Indeed, here we have only one level crossing and improvement of the adiabaticity in the resonance leads to stronger transition. With the increase of Δm_{02}^2, and therefore R_Δ, the dip moves to high energies but the resonance shifts to higher densities, i.e., to the central regions of the Sun where the density gradient is smaller and adiabaticity is better. Here, substantial change of the probability exists for smaller mixing angles.

If $m_0 < m_1 < m_2$, so that $\Delta m_{01}^2 < 0$, the sterile level λ_s crosses $\nu_{1m}^{\rm LMA}$ at high densities only

$$n_h^R \approx 2n^{\rm LMA}(1 + R_\Delta).$$

The resonance energy equals

$$E \approx E_R^{\rm LMA} \frac{2n_e}{n_n},$$

where n_n is the number density of neutrons. In this case we have the same general expressions for the survival probability as in (20) and (21). Consequently, the expressions for P_{ee} in the adiabatic and nonadiabatic limits coincide with those (see e.g. (25)) for one sterile resonance. However, the dip here is at high energies.

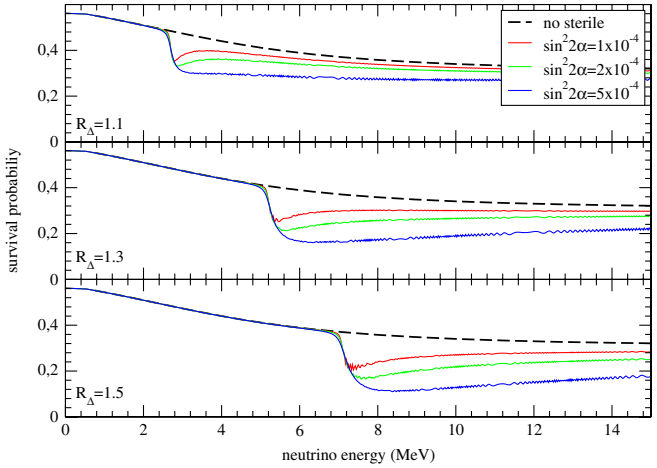

FIG. 13 (color online). The same as in Fig. 3 for $R_\Delta > 1$.

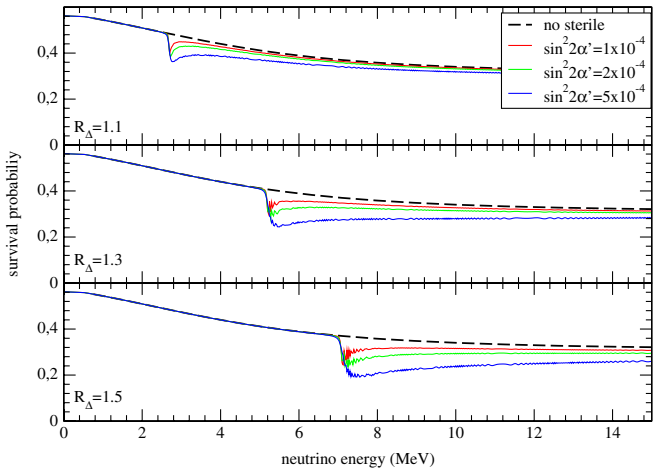

FIG. 14 (color online). The same as in Fig. 4 for $R_\Delta > 1$ and ν_s mixing in ν_2.

In the case of flavor mixing, that is, the mixing of ν_s with ν_e, ν_a the matrices U_θ and U_α should be permuted, so that $U^{(3)} = U_\alpha U_\theta$ (compare with (7)). It can be shown that now the off-diagonal elements of the Hamiltonian H_α contain terms with Δm_{01}^2 and Δm_{02}^2 simultaneously. As a result, the probabilities have energy dependences which are intermediate between those for mixings in mass states ν_1 and ν_2.

[1] L. Wolfenstein, Phys. Rev. D **17**, 2369 (1978); in *Neutrino'78, 8th International Conference on Neutrino Physics and Astrophysics*, edited by E. C. Fowler (Purdue University Press, West Lafayette, 1978), p. C3.
[2] S. P. Mikheyev and A. Yu. Smirnov, Sov. J. Nucl. Phys. **42**, 913 (1985); Nuovo Cimento Soc. Ital. Fis. C **9**, 17 (1986); Zh. Eksp. Teor. Fiz. **91**, 7 (1986) [Sov. Phys. JETP **64**, 4 (1986)].
[3] B. T. Cleveland *et al.*, Astrophys. J. **496**, 505 (1998).
[4] J. N. Abdurashitov *et al.* (SAGE Collaboration), Phys. Rev. C **80**, 015807 (2009).

[5] M. Altmann *et al.* (GNO Collaboration), Phys. Lett. B **616**, 174 (2005).
[6] J. Hosaka *et al.* (Super-Kamkiokande Collaboration), Phys. Rev. D **73**, 112001 (2006).
[7] B. Aharmim *et al.* (SNO Collaboration), Phys. Rev. C **72**, 055502 (2005).
[8] B. Aharmim *et al.* (SNO Collaboration), Phys. Rev. C **75**, 045502 (2007).
[9] B. Aharmim *et al.* (SNO Collaboration), Phys. Rev. Lett. **101**, 111301 (2008).
[10] C. Arpesella *et al.* (The Borexino Collaboration), Phys. Rev. Lett. **101**, 091302 (2008).
[11] S. Abe *et al.* (KamLAND Collaboration), Phys. Rev. Lett. **100**, 221803 (2008).
[12] A. Gando *et al.*, Phys. Rev. D **83**, 052002 (2011).
[13] P. C. de Holanda and A. Y. Smirnov, Phys. Rev. D **69**, 113002 (2004).
[14] M. Cirelli, G. Marandella, A. Strumia, and F. Vissani, Nucl. Phys. **B708**, 215 (2005).
[15] K. Abe *et al.*, Phys. Rev. D **83**, 052010 (2011).
[16] B. Aharmim *et al.* (SNO Collaboration), Phys. Rev. C **81**, 055504 (2010).
[17] G. Bellini *et al.* (The Borexino Collaboration), Phys. Rev. D **82**, 033006 (2010).
[18] E. Komatsu *et al.*, Astrophys. J. Suppl. Ser. **192**, 18 (2011).
[19] J. Dunkley *et al.*, arXiv:1009.0866.
[20] J. Hamann, S. Hannestad, G. G. Raffelt, I. Tamborra, and Y. Y. Y. Wong, Phys. Rev. Lett. **105**, 181301 (2010).
[21] U. Seljak, A. Slosar, and P. McDonald, J. Cosmol. Astropart. Phys. 10 (2006) 014.
[22] Y. I. Izotov and T. X. Thuan, Astrophys. J. **710**, L67 (2010).
[23] G. Steigman, J. Cosmol. Astropart. Phys. 04 (2010) 029; E. Aver, K. A. Olive, and E. D. Skillman, J. Cosmol. Astropart. Phys. 05 (2010) 003; J. Cosmol. Astropart. Phys. 03 (2011) 043.
[24] L. M. Krauss, C. Lunardini, and C. Smith, arXiv:1009.4666; K. Nakayama, F. Takahashi, and T. T. Yanagida, Phys. Lett. B **697**, 275 (2011).
[25] J. N. Bahcall, S. Basu, M. Pinsonneault, and A. Serenelli, Astrophys. J. **618**, 1049 (2005); N. Grevesse and A. J. Sauval, Space Sci. Rev. **85**, 161 (1998); A. M. Serenelli, Astrophys. Space Sci. **328**, 13 (2009).
[26] Y. Kishimoto (KamLAND Collaboration), J. Phys. Conf. Ser. **120**, 052010 (2008).
[27] M. C. Chen (SNO+ Collaboration), arXiv:0810.3694; C. Kraus and S. J. M. Peeters (SNO+ Collaboration), Prog. Part. Nucl. Phys. **64**, 273 (2010).
[28] P. Adamson *et al.* (MINOS Collaboration), arXiv:1104.3922; Phys. Rev. D **81**, 052004 (2010).
[29] A. D. Dolgov and F. L. Villante, Nucl. Phys. **B679**, 261 (2004).
[30] A. Donini, M. Maltoni, D. Meloni, P. Migliozzi, and F. Terranova, J. High Energy Phys. 12 (2007) 013.
[31] O. Schulz (IceCube Collaboration), AIP Conf. Proc. **1085**, 783 (2009); C. Wiebusch (f. t. I. Collaboration), arXiv:0907.2263.
[32] P. C. de Holanda and A. Yu. Smirnov (unpublished).